



## ARTICLE

# A homozygous structural variant of *RPGRIP1* is frequently associated with achromatopsia in Japanese patients with IRD



Akiko Suga<sup>1</sup>, Kei Mizobuchi<sup>2</sup>, Taiga Inooka<sup>3</sup>, Kazutoshi Yoshitake<sup>4</sup>, Naoko Minematsu<sup>1</sup>, Kazushige Tsunoda<sup>5</sup>, Kazuki Kuniyoshi<sup>6</sup>, Yosuke Kawai<sup>7</sup>, Yosuke Omae<sup>7</sup>, Katsushi Tokunaga<sup>7</sup>, NCBN Controls WGS Consortium, Takaaki Hayashi<sup>2,\*</sup>, Shinji Ueno<sup>8,\*</sup>, Takeshi Iwata<sup>1,\*</sup>

## ARTICLE INFO

*Article history:*

Received 16 October 2023

Received in revised form

21 March 2024

Accepted 21 March 2024

Available online 26 March 2024

*Keywords:*

Achromatopsia

Genome sequencing

RPGRIP1

Structural variant

## ABSTRACT

**Purpose:** Achromatopsia (ACHM) is an early-onset cone dysfunction caused by 5 genes with cone-specific functions (*CNGA3*, *CNGB3*, *GNAT2*, *PDE6C*, and *PDE6H*) and by *ATF6*, a transcription factor with ubiquitous expression. To improve the relatively low variant detection ratio in these genes in a cohort of exome-sequenced Japanese patients with inherited retinal diseases (IRD), we performed genome sequencing to detect structural variants and intronic variants in patients with ACHM.

**Methods:** Genome sequencing of 10 ACHM pedigrees was performed after exome sequencing. Structural, non-coding, and coding variants were filtered based on segregation between the affected and unaffected in each pedigree. Variant frequency and predicted damage scores were considered in identifying pathogenic variants.

**Results:** A homozygous deletion involving exon 18 of *RPGRIP1* was detected in 5 of 10 ACHM probands, and variant inheritance from each parent was confirmed. This deletion was relatively frequent (minor allele frequency = 0.0023) in the Japanese population but was only homozygous in patients with ACHM among the 199 Japanese IRD probands analyzed by the same genome sequencing pipeline.

**Conclusion:** The deletion involving exon 18 of *RPGRIP1* is a prevalent cause of ACHM in Japanese patients and contributes to the wide spectrum of *RPGRIP1*-associated IRD phenotypes, from Leber congenital amaurosis to ACHM.

© 2024 The Authors. Published by Elsevier Inc. on behalf of American College of Medical Genetics and Genomics. This is an open access article under the CC BY-NC-ND license (<http://creativecommons.org/licenses/by-nc-nd/4.0/>).

The Article Publishing Charge (APC) for this article was paid by Takeshi Iwata

Akiko Suga and Kei Mizobuchi contributed equally to this article.

The names of the NCBN Controls WGS Consortium will appear at the end of the article.

\*Correspondence and requests for materials should be addressed to Takeshi Iwata, Division of Molecular and Cellular Biology, National Institute of Sensory Organs, NHO Tokyo Medical Center, 2-5-1, Higashigaoka Meguro-ku, Tokyo 152-8902 Japan. *Email address:* [takeshi.iwata@kankakuki.jp](mailto:takeshi.iwata@kankakuki.jp) OR Takaaki Hayashi, Department of Ophthalmology, The Jikei University School of Medicine, 3-25-8 Nishi-shimbashi, Minato-ku, Tokyo 105-8461, Japan. *Email address:* [taka@jikei.ac.jp](mailto:taka@jikei.ac.jp) OR Shinji Ueno, Department of Ophthalmology, Hirosaki University Graduate School of Medicine, 5 Zaifu-cho Hirosaki-shi, Aomori 036-8562, Japan. *Email address:* [uenos@hirosaki-u.ac.jp](mailto:uenos@hirosaki-u.ac.jp)

Affiliations are at the end of the document.

doi: <https://doi.org/10.1016/j.gimo.2024.101843>

2949-7744/© 2024 The Authors. Published by Elsevier Inc. on behalf of American College of Medical Genetics and Genomics. This is an open access article under the CC BY-NC-ND license (<http://creativecommons.org/licenses/by-nc-nd/4.0/>).

## Introduction

Inherited retinal diseases (IRDs) are a group of phenotypes associated with reduced visual acuity and are mostly due to a photoreceptor dysfunction, which leads to progressive retinal degeneration. Achromatopsia (ACHM) is a congenital cone dysfunction with severely reduced visual acuity but a stationary natural history from an early age. Affected patients have nystagmus, photophobia, absent or markedly reduced color vision, and reduced visual acuity from birth or early infancy. With electroretinography (ERG), ACHM is characterized by severely reduced cone responses with normal/subnormal rod responses. The fundus typically appears normal, but detailed imaging of the retinal structure with optical coherence tomography (OCT) reveals variability in the macular structure, with an ellipsoid zone that is either continuous or disrupted.<sup>1</sup> Long-term clinical studies indicate that visual acuity, rod responses, and retinal structure are generally stable for several years to decades.<sup>2</sup> ACHM is inherited in an autosomal recessive pattern with a prevalence of 1 in 30,000 worldwide.<sup>3</sup> Six genes, *CNGA3* (HGNC:2150, NM\_001298.2), *CNGB3* (HGNC:2153, NM\_019098.5), *GNAT2* (HGNC:4394, NM\_001377295.2), *PDE6C* (HGNC:8787, NM\_006204.4), *PDE6H* (HGNC:8790, NM\_006205.3), and *ATF6* (HGNC:791, NM\_007348.4), are causal for ACHM.<sup>2</sup> *ATF6* is ubiquitously expressed and involved in the maintenance of cellular homeostasis, whereas the remaining genes encode cone-specific phototransduction proteins.<sup>4</sup> Genetic studies on patients with IRD have shown relatively high solved ratios for ACHM. For example, 67% (6/9 cases) of the patients with ACHM were solved by genome sequencing in the United Kingdom,<sup>5</sup> and 95.2% (56/62 cases) were solved by the panel sequencing of known IRD genes in Germany.<sup>6</sup> Even with Sanger sequencing targeting the coding sequences of *CNGA3* and *CNGB3*, biallelic variants were detected in 45.5% (10/22 pedigrees) of the patients with ACHM.<sup>7</sup> Consistent with the known genetic background of ACHM; *CNGB3* and *CNGA3* account for approximately 70% to 80% of the cases.<sup>2</sup> Those studies identified *CNGB3* as the most frequent causal gene and its founder variant, c.1148del p.(Thr383Ilefs\*13), as the most prevalent. In contrast, in the previous exome sequencing of 1210 Japanese IRD pedigrees, we identified pathogenic variants in only 34% of the pedigrees with cone dysfunction (14/41 pedigrees, including ACHM and blue cone monochromatism).<sup>8</sup> Among the patients with genetically solved cone dysfunction, *CNGA3* accounted for 22% (3/14) but *CNGB3* did not. Further, the *CNGB3* founder variant, c.1148del, was not detected in the exome-sequenced patients with IRD either in a heterozygous or in a homozygous manner. Therefore, we expected a contribution of exome-undetectable structural variants and non-coding variants in known ACHM genes and/or other genes in Japanese patients with ACHM.

*RPGRIP1* (HGNC:13436, NM\_020366.4) encodes a coiled-coil protein that interacts with the RPGR protein and anchors it to the photoreceptor primary cilia.<sup>9</sup> A pathogenic variant of *RPGRIP1* was first identified in patients with

Leber congenital amaurosis (LCA) with severely reduced vision from early childhood, pigmented fundi, and non-recordable ERGs for both rod and cone responses.<sup>10</sup> Over 250 variants of *RPGRIP1* are currently known, most of which are associated with LCA; associations with retinitis pigmentosa and cone-rod dystrophy (CORD) are observed at lower rates.<sup>11</sup> Although *RPGRIP1* pathogenic variants may underlie 5% of LCA cases,<sup>12</sup> our previous exome sequencing study did not identify *RPGRIP1* pathogenic variants in patients with any of the 28 phenotypes, including LCA (54 pedigrees) and CORD (157 pedigrees).<sup>8</sup> Recent next-generation sequencing efforts have identified pathogenic non-coding variants and large structural variants partially disrupting *RPGRIP1* exon(s) in patients with IRD,<sup>13</sup> which encouraged us to reexamine unresolved IRD cases with genome sequencing to detect structural variants and noncoding variants in addition to the coding region variants detected by exome sequencing.

Herein, we report the identification of a homozygous deletion involving exon 18 of *RPGRIP1* (NC\_000014.9:g.21326547\_21327885del NM\_020366.4:c.2710+374\_2895+78del; *RPGRIP1*-ex18-DEL) in 5 of 10 clinically diagnosed unrelated ACHM probands in the Japanese IRD cohort. These patients had severely reduced visual acuity from birth or early infancy, and ERG responses were normal from rods but nonrecordable from cones. Genome sequencing revealed that *RPGRIP1*-ex18-DEL was homozygous in the patients and heterozygous in their parents. It was significantly enriched in patients with ACHM compared with the Japanese control population, accounting for 11% of pedigrees with cone dysfunction syndrome in our exome-sequenced and genome-sequenced Japanese IRD cohort.

## Materials and Methods

### Recruitment of patients and their family members

Ten clinically diagnosed ACHM probands and their family members (2 affected and 19 unaffected) were enrolled in this study at 4 institutions in Japan (NHO Tokyo Medical Center, The Jikei University School of Medicine, Nagoya University, and Kindai University). These participants were part of a genome-sequenced IRD cohort (199 pedigrees, [Supplemental Figure 1](#)) collected by the Japan Eye Genetics Consortium.<sup>14</sup> Recruitment and sample collection were conducted in accordance with the Declaration of Helsinki. All participants provided written informed consent at their respective recruiting institutes. The study was approved by the ethics boards of each institute.

### Clinical evaluation

We performed comprehensive ophthalmic examinations, including medical review (age at onset and chief complaint),

decimal best-corrected visual acuity (BCVA), fundus photographs, fundus autofluorescence imaging using a Spectralis HRA (Heidelberg Engineering) and/or Optos 200Tx/California Ultra-Wide Field Retinal Imaging System (Optos), OCT (Spectralis, or Carl Zeiss Meditec AG), and Goldmann kinetic perimetry (Haag Streit). Full-field ERG was recorded following the protocols of the International Society for Clinical Electrophysiology of Vision (ISCEV)<sup>15</sup> using a light-emitting diode built-in electrode (LE-4000, Tomey), a Ganzfeld dome with an EOG-ERG Ganzfeld stimulator (Electrophysiology system; LACE Elettronica), or RETeval (LKC Technologies). Detailed ERG procedures and conditions were as previously reported.<sup>16-19</sup> Pedigree trees were drawn by f-tree (v4.2.1).<sup>20</sup>

## Genome sequencing

Blood samples were collected at each institute, and genomic DNA was extracted by Advanced GenoTechs. All patients and healthy controls were genome sequenced by the same pipeline as part of the Japan Leading Project for Rare Disease WGS.<sup>21,22</sup> In detail, genome sequencing was performed using NovaSeq6000 (Illumina) at 150 bp paired-end. Sequences in FASTQ data are mapped to a GRCh38 reference sequence by an in-house data analysis pipeline<sup>21</sup> equivalent to bwa (v0.7.15)<sup>23</sup> and GATK (v4.1.0).<sup>24</sup> The mapping and variant calls were performed using the Parabricks v3.5.0 (Nvidia). Mapped sequence files were used for variant calling by our in-house pipeline. In detail, short sequence variants (single-nucleotide variants [SNVs] and insertions/deletions shorter than 50 bp [short indels]) were called by a GATK-haplotype caller as previously reported.<sup>8</sup> Variants were annotated by ANNOVAR (2019Oct24)<sup>25</sup> and Splice AI (1.3).<sup>26</sup> For the detection of structural variants, sequences were processed by GATK-SV (v0.12-beta)<sup>27</sup> using the single mode with MELT (v2.2.2).<sup>28</sup>

## Variant filtration and interpretation

To identify pathogenic variants in each patient with IRD, we used pedigree-based variant segregation as previously reported.<sup>8</sup> SNVs and short indels in known IRD causal genes (Supplemental Table 1) were examined. Variants with a minor allele frequency (MAF) <0.005 in gnomAD and 8.3 KJPN and frequent population-specific variants in *EYS* (NM\_001142800.2:c.2528G>A, MAF =  $1.89 \times 10^{-2}$  in 8.3 KJPN) and *RP1* (NM\_006269.2:c.5797C>T, MAF =  $5.40 \times 10^{-3}$  in 8.3 KJPN) were considered. The MAFs of structural variants were referenced to gnomAD-SV (v.2.1), 8.3 KJPN-SV,<sup>29</sup> and NCBN Controls WGS.<sup>21</sup> Variants were segregated between the affected and unaffected in each family as follows. For pedigrees with dominant inheritance of the phenotype, variants shared only among patients were selected. For pedigrees comprising the patient and his or her unaffected family members, recessive, X-linked, and sporadic inheritance patterns were considered. Variants were selected if they were homozygous or heterozygous in patient(s) but not

homozygous in unaffected family members. Compound heterozygosity was examined if each parent carried different alleles. For pedigrees comprising only probands, all genotypes were considered. The pathogenicity of short-read variants and structural variants was predicted according to the American College of Medical Genetics and Genomics guidelines using InterVar<sup>30</sup> and AnnotSV,<sup>31</sup> respectively.

Short-read mapping was confirmed with integrated genome visualization software (IGV, v2.1.6).<sup>32</sup>

## Confirmation of the break point

*RPGRIP1*-exon18-DEL was confirmed by polymerase chain reaction (PCR) and Sanger sequencing using previously reported primers for PCR (Fw: 5'-GAGCCCGAGTGCCTTTACTG-3'; Rv: 5'-CCAGCTTCAATGGGAACCTC-3'),<sup>33</sup> and nested primers for sequencing (Fw: 5'-TTGCCCAGGCTAGTAGCTGGG-3'; Rv: 5'-TTC AAGTGATTCTCCTGCC TC-3'). The break-point sequence of *RPGRIP1* exon 22-24 DUP was confirmed by PCR amplification and Sanger sequencing (primers Fw: 5'-TGTGGCAGATCCTGGA GTCA-3'; Rv: 5'-GCAGGGCTGCCAAAACCTTAC-3').

To confirm the break-point sequence of *CNGA3* *Alu* insertion, PCR-amplified target region was subcloned into pMD20 by TA-cloning (Mighty TA-cloning Reagent Set for PrimeSTAR, TAKARA) and Sanger sequenced. The following primers were used for PCR amplification and sequencing (Fw: 5'-GATGCCCAATGACCTCCATCTT-3'; Rv: 5'-GGTAAGGGTCAAGGTGGACCAG-3'). The subfamily of the inserted *Alu* sequence was annotated by Dfam.<sup>34</sup>

## Statistical analysis

The enrichment of *RPGRIP1*-ex18-DEL in the ACHM probands was examined by a one-sided binominal test using rstatix (0.7.2) on R (4.2.3).

## Results

### Clinical findings

Table 1 summarizes the clinical findings from 8 patients with biallelic *RPGRIP1* structural variants. All patients were diagnosed with ACHM based on medical review, visual acuity, retinal structure, and functional findings. Detailed clinical findings from a representative patient (JU0960) are shown in Figure 1. Multimodal retinal imaging revealed a normal appearance by fundus photograph and fundus autofluorescence imaging (Figure 1A, upper 3 panels) and blurred outer retinal layers (including the ellipsoid zone) by OCT (Figure 1A, lower panels). Full-field ERG showed normal rod system function (Figure 1B, dark adapted [DA] 0.01) and combined rod and cone system functions (Figure 1B, DA 3.0 and DA 10.0), with severely impaired

**Table 1** Summary of the clinical findings of patients with ACHM with *RPGRIP1* exon18 deletion

Case		Subjective Symptom					BCVA (logMAR)		Visual Field Test					
Family ID <sup>a</sup>	Patient ID	Age <sup>b</sup>	Gender	Nystagmus	Photophobia	Color Vision Abnormality	RE	LE	Fundus Photograph	FAF	OCT	FF-ERG <sup>c</sup>	Central	Peripheral
N051	N1051	21	M	+	+	+	0.40	0.52	Normal appearance	Normal appearance	Blurred EZ appearance	Rod: subnormal Rod & cone: decreased a- and b-waves Cone: non-recordable 30-Hz flicker: non-recordable	Relative central scotoma of I-4e	Constricted
	N0051	24	F	+	+	+	1.00	1.00	Normal appearance	Normal appearance	Normal appearance	Rod; normal Rod & cone: normal a- and b-waves cone: non-recordable 30-Hz flicker: non-recordable	Noncentral scotoma	Constricted
N058	N0058	39	F	+	+	+	1.52	1.70	Normal appearance	Normal	Blurred EZ	Rod; normal Rod & cone: normal a- and b-waves cone: non-recordable 30-Hz flicker: non-recordable	Relative central scotoma of III-4e in RE and II-4e in LE	Constricted
NISO 199	KA-199	35	F	+	+	+	1.10	1.10	Macular atrophy	Hypo-AF corresponding to macular atrophy area	Disrupted EZ corresponding to macular atrophy area	Rod; normal Rod & cone: normal a- and b-waves cone: non-recordable 30-Hz flicker: non-recordable	Relative central scotoma of I-4e	Constricted
							1.10	1.10	Normal appearance	Normal appearance	Blurred EZ	Rod; normal Rod & cone: normal a- and b-waves cone: non-recordable 30-Hz flicker: non-recordable	Noncentral scotoma	Preserved
J134	JU0960	5	M	+	+	+	0.82	1.00	Normal appearance	Normal appearance	Blurred EZ	Rod; normal Rod & cone: normal a- and b-waves cone: non-recordable 30-Hz flicker: non-recordable	Relative central scotoma of I-3e	Preserved
J138	JU0011	24	M	+	+	+	1.15	1.00	Normal appearance	Hypo-AF at fovea and hyper-AF around the area	Blurred EZ at fovea and disrupted EZ at parafovea	Rod; normal Rod & cone: normal a- and b-waves cone: non-recordable 30-Hz flicker: non-recordable	Relative central scotoma of I-3e	Preserved
NISO 143	KA-143	21	F	+	+	+	1.52	1.52	Normal appearance	Not Done	Blurred EZ	Rod; normal Rod & cone: slightly decreased a- and normal b-waves cone: non-recordable 30-Hz flicker: non-recordable	Not Done	

<sup>a</sup>J, The Jikei University School of Medicine; N, Nagoya university; NISO, NHO Tokyo Medical Center.

<sup>b</sup>Age, age at first visit; *BCVA*, best-corrected visual acuity; *DA*, dark adapted; *EZ*, ellipsoid zone; *FAF*, fundus autofluorescence imaging; *FF-ERG*, full-field electroretinogram; *LA*, light adapted; *LE*, left eye; *OCT*, optical coherence tomography; *RE*, right eye.

<sup>c</sup>Rod, DA 0.01, Rod and cone (DA 3.0 or DA 10); Cone, (LA 3.0); 30-Hz flicker, (LA 3.0-flicker).



cone function (Figure 1B, light adapted [LA] 3.0 and LA 3.0 flicker). The clinical course of visual acuity in the patient revealed that the logMAR BCVA remained around 1.0 for about 15 years (Figure 1C). These findings are consistent with the ACHM phenotype.

### Detection of homozygous *RPGRIP1* SV in Japanese patients with achromatopsia

These 10 ACHM pedigrees were previously analyzed by exome sequencing, but no pathogenic variants with homozygous or compound heterozygous genotypes were identified. Genome sequencing detected homozygous *RPGRIP1*-ex18-DEL, in 5 of 10 unrelated ACHM probands (Figure 2A and B, Table 2). These pedigrees were genome sequenced as complete trios (proband and their healthy parents), except for the father of N058, and variant inheritance was traced by genotype. A homozygous 1339-bp deletion in probands was confirmed by Sanger sequencing (Figure 2C) following PCR amplification of the target region (Supplemental Figure 2). This variant was previously reported as a deletion of exon 17 in a Japanese patient with LCA.<sup>33</sup> Annotation of the exon number changed according to the recent identification of a new exon corresponding to the 5'UTR.<sup>13</sup> Although *RPGRIP1*-ex18-DEL was predicted to cause premature termination of the *RPGRIP1* protein (NP\_065099.3:p.(Asp905Serfs\*6)),<sup>33</sup> its exact effect on transcripts and proteins has yet to be experimentally confirmed. Two other ACHM probands were heterozygous for *RPGRIP1*-ex18-DEL (Table 2, JU0011 and KA-143), and 1 of these patients had a previously reported *RPGRIP1* nonsense variant<sup>35</sup> *in trans* (Figure 2D and E).

Another proband had a novel partial duplication of *RPGRIP1* coding exons (NC\_000014.9: g.21338066\_21348664\_dup NM\_020366.4:c.3339+3361\_3748+362dup; *RPGRIP1* ex22-24 DUP) *in trans* (Figure 3A and B). Genomic PCR confirmed the heterozygosity of the *RPGRIP1*-ex18-DEL in I-2 and II-1, and the *RPGRIP1* ex22-24 DUP in I-1 and II-1, respectively (Figure 3C). The break point of the duplicated region was revealed by Sanger sequencing (Figure 3D).

To examine the contribution of *RPGRIP1*-ex18-DEL to ACHM in association with other ACHM causal genes, we reviewed rare SNVs (population-maximum MAF < 0.005 in gnomAD) in *CNGA3*, *CNGB3*, *GNAT2*, *PDE6C*, *PDE6H*, and *ATF6* for all these patients. No heterozygous or homozygous pathogenic or likely pathogenic ClinVar variants were detected. NISO472 II-1 was heterozygous for *CNGA3*: p.(Asp193Asn), which was of uncertain significance.

In the other 3 ACHM pedigrees, no *RPGRIP1* pathogenic variant was detected. We identified a *CNGA3* missense variant, c.1072G>A p.(Glu358Lys), and an *Alu* insertion as a compound heterozygous genotype in NISO177 (Table 2). A 356 bp *AluY* insertion with 18 bp target site duplication was shown by Sanger sequencing following the TA-cloning of the target region amplified by PCR (Supplemental Figure 3). Both variants were of uncertain significance, and further validation

was required. No pathogenic/candidate pathogenic variants were detected in the other 2 pedigrees.

In total, genome sequencing identified homozygous *RPGRIP1*-ex18-DEL in 5 of 10 (50%) ACHM probands, and *RPGRIP1*-ex18-DEL *in trans* with other *RPGRIP1* nonsense/truncating variants in 2 ACHM probands (20%, 2/10) (Table 2).

### Enrichment of homozygous *RPGRIP1*-exon18-DEL in achromatopsia

Compared with the general MAF of *RPGRIP1*-ex18-DEL in the Japanese population (0.0023, 1/444 in 8.3 KJPN), the MAF = 0.60 (12/20) in our 10 ACHM probands was extremely high ( $P = 4.74 \times 10^{-24}$ , one-sided binominal test). To determine if this variant was prevalent among Japanese patients with IRD independent of the phenotype, we reviewed the *RPGRIP1*-ex18-DEL genotype for all genome-sequenced IRD probands (Supplemental Figure 1,  $n = 199$ ). Homozygous *RPGRIP1*-ex18-DEL was found only in the 5 previously mentioned ACHM patients (Table 2). Heterozygous *RPGRIP1*-ex18-DEL was found in 2 ACHM patients (Table 2) and 2 additional patients diagnosed with LCA. These patients with LCA were from the same family, and both had another structural variant (NC\_000014.9:g.21276147\_21280265del; *RPGRIP1*-ex1-DEL) *in trans*. Their detailed phenotypes were reported recently.<sup>36</sup>

## Discussion

In our genome sequencing analysis of 10 ACHM pedigrees, 5 probands were homozygous for the same pathogenic variant, *RPGRIP1*-ex18-DEL. No other probands in our genome-sequenced IRD cohort ( $n = 199$ ) were homozygous for this variant, indicating that homozygous *RPGRIP1*-ex18-DEL primarily accounts for ACHM.

Ophthalmic examinations revealed a typical ACHM phenotype among the patients, including symptoms of nystagmus, photophobia, color vision abnormality, and stable visual acuity after initial severe reduction. In addition to the detailed phenotype of JU0960 in this report, phenotypes of N1051 and N0051 were previously reported as ACHM and incomplete ACHM, respectively, before the genetic examination.<sup>37</sup> A normal fundus photograph and normal rod function with severely impaired cone function are characteristic of ACHM, rather than LCA.<sup>2</sup> Biallelic *RPGRIP1* variants are mainly associated with an LCA phenotype.<sup>10</sup> However, some IRD cases with *RPGRIP1* pathogenic variants have been clinically diagnosed as CORD in variable regions and populations.<sup>11,38</sup> In addition, in studies of Japanese patients with LCA with *RPGRIP1* variants, cases with heterozygous *RPGRIP1*-ex18-DEL were notable for the lack of general fundus abnormality and subnormal rod ERG responses with unrecordable cone responses.<sup>36,39</sup> Furthermore, in the initial report of *RPGRIP1*-ex18-DEL (mentioned as exon 17

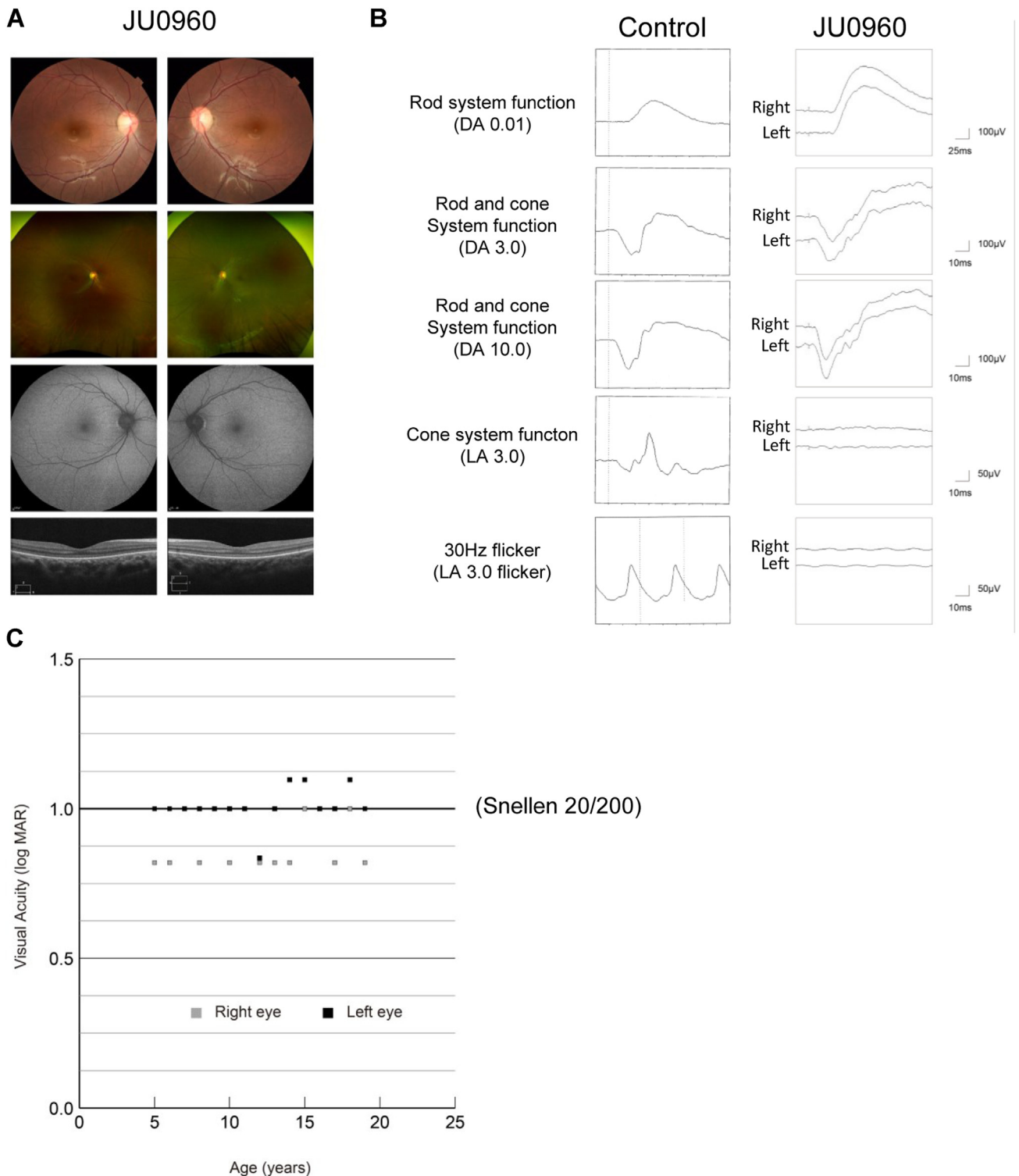


**Figure 1 Clinical findings from a representative patient (JU0960).** A. Multimodal retinal imaging showed a normal appearance by fundus photograph (first and second panels) and fundus autofluorescence imaging (third panel) and blurred outer retinal layer ellipsoid zone by OCT (fourth panel). B. Full-field electroretinography showed normal rod system function (DA 0.01) and combined rod and cone system functions (DA 3.0 and DA 10.0) with unrecordable cone system function (LA 3.0) and 30-Hz flicker responses (LA 3.0 flicker). C. The clinical course of visual acuity revealed that logMAR BCVA remained around 1.0 for about 15 years.

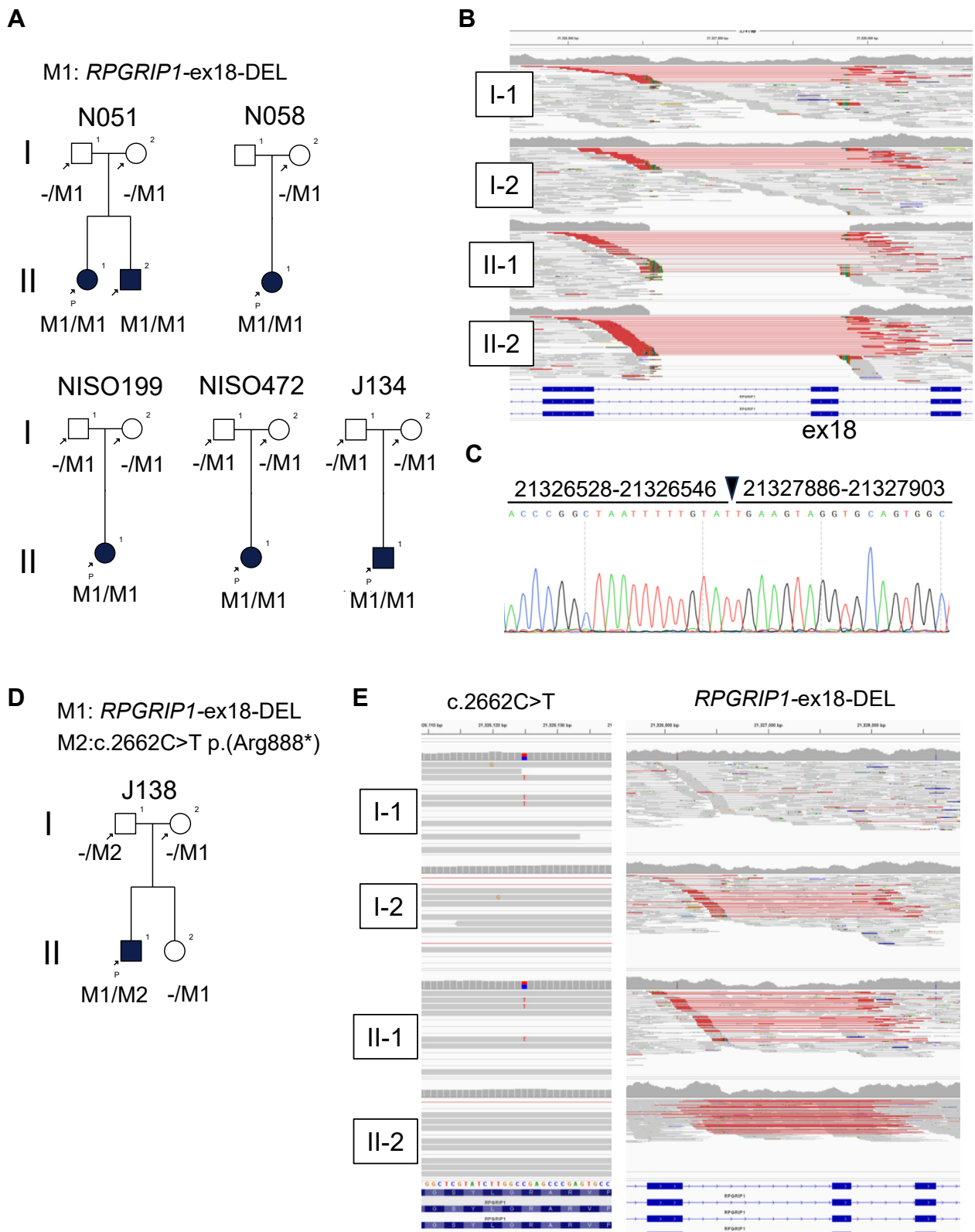


**Figure 2 Identification of *RPGRIP1*-ex18-DEL in ACHM proband.** A. Family trees of the patients with ACHM (black) and their healthy parents (white). B. Read alignments of N051 displayed by IGV. Red lines indicate deletions in the read sequences compared with the reference. C. Sanger sequencing identifies the exact break point (black arrowhead) using the PCR product of N051 II-1. Chromosomal position based on NC\_000014.9 (hg38) is indicated. D. Family tree of JIKEI138 showing variant inheritance of *RPGRIP1*-ex18-DEL and c.2662C>T. E. Read alignments showing c.2662C>T and *RPGRIP1*-ex18-DEL. Clinically examined and genome-sequenced participants are indicated by arrows. Probands are indicated by P, males are indicated by rectangles, and females are indicated by circles.

**Table 2** Overview of molecular findings of genome-sequenced patients with achromatopsia

IDs	Pathogenic Variant				Population Frequency				Prediction of Pathogenicity									
	Family	Patient	Gene	Genotype	g.notation(hg38)	c.notation	p.notation	gnomAD (max)	gnomAD (EAS)	ExAC (All)	8.3KJPN	Variant Class (ACMG)	PolyPhen2	SIFT	REVEL	VEST4	ClinVar	Reference
N051	1051	<i>RPGRIP1</i>	Homozygous	g.21326547_21327885del	c.2710+374_2895+78del	p.?	NA	NA	NA	0.0023	Pathogenic (Class 5)							33
		<i>RPGRIP1</i>	Homozygous	g.21326547_21327885del	c.2710+374_2895+78del	p.?	NA	NA	NA	0.0023	Pathogenic (Class 5)							33
N058	0058	<i>RPGRIP1</i>	Homozygous	g.21326547_21327885del	c.2710+374_2895+78del	p.?	NA	NA	NA	0.0023	Pathogenic (Class 5)							33
		<i>RPGRIP1</i>	Homozygous	g.21326547_21327885del	c.2710+374_2895+78del	p.?	NA	NA	NA	0.0023	Pathogenic (Class 5)							33
N199	KA-472	<i>RPGRIP1</i>	Homozygous	g.21326547_21327885del	c.2710+374_2895+78del	p.?	NA	NA	NA	0.0023	Pathogenic (Class 5)							33
		<i>RPGRIP1</i>	Homozygous	g.21326547_21327885del	c.2710+374_2895+78del	p.?	NA	NA	NA	0.0023	Pathogenic (Class 5)							33
J134	JU0960	<i>RPGRIP1</i>	Homozygous	g.21326547_21327885del	c.2710+374_2895+78del	p.?	NA	NA	NA	0.0023	Pathogenic (Class 5)							33
		<i>RPGRIP1</i>	Compound heterozygous	chr14:g.21326125C>T	c.2662C>T	p.(Arg888*)	0.00003425	0	NA	0.000155	Likely pathogenic (Class 4)	NA	Tolerant	NA	0.754	VUS		35
N150	KA-143	<i>RPGRIP1</i>	Compound heterozygous	g.21326547_21327885del	c.2710+374_2895+78del	p.?	NA	NA	NA	0.0023	Pathogenic (Class 5)							33
		<i>RPGRIP1</i>	Compound heterozygous	chr14:g.21338066_21348664_dup	c.3339+3361_3748+362dup	p.?	NA	NA	NA	NA	NA	VUS (Class 3)						novel
N177	KA-178	<i>CMGA3</i>	Compound heterozygous	g.98396296G>A	c.1126G>A	p.(Glu376Lys)	0.000008838	0	NA	0	VUS (Class 3)	Benign	Tolerant	0.517	0.524	NA		novel
		<i>CMGA3</i>	Compound heterozygous	g.98396034_98396035insN[356]	c.864_865insN[356]	p.?	NA	NA	NA	NA	NA	VUS (Class 3)						novel

Variant descriptions for *RPGRIP1* are based on NC\_000014.9 for g.notation and NM\_020366.4 for c.notation. Variant descriptions for *CMGA3* are based on NC\_000002.12 for g.notation and NM\_001298.2 for c.notation.

VUS, variants with uncertain significance.

deletion) from Japanese patients with LCA, the authors noted that 1 patient had recordable scotopic ERG with unrecordable cone response at 5 years old.<sup>33</sup> Considering our data and previous studies on *RPGRIP1*-associated IRD phenotypes, *RPGRIP1* may be causal for a spectrum of photoreceptor-associated phenotypes, from functional defects primarily in cones (ACHM and CORD) to photoreceptor degeneration in both rods and cones (LCA and early-onset retinitis pigmentosa). Further studies on structural variants and SNVs will reveal the correlations between these genetic variants and phenotypes.

In our previous exome sequencing report, population-frequent SNVs of *EYS* (NM\_001142800.2:c.2528G>A) and *RPI* (NM\_006269.2:c.5797C>T) were significantly enriched in retinitis pigmentosa and macular dystrophy/CORD, respectively.<sup>8</sup> In this report, using genome sequencing, we show that *RPGRIP1*-ex18-DEL was significantly enriched in ACHM in the Japanese population, with the homozygous genotype mainly accounting for the phenotype. This variant was not detected in gnomAD structural variants (v2.1); therefore, it was difficult to determine the contribution of population-frequent structural variants to ACHM. However, the relatively high variant frequency in the Japanese population (MAF = 0.0023 in 8.3 KJPN) supported this idea. A further expansion of publicly available structural variant data will enable us to compare the prevalence of SVs and SV-associated IRDs between countries and populations. Our data suggest that genome sequencing is effective in detecting a relatively small deletion, such as *RPGRIP1*-ex18-DEL (1339bp). Although the depletion of exon 18 in *RPGRIP1* was detectable by the read alignment of exome sequencing (Supplemental Figure 4a), no information about the break point was available. Furthermore, the read counts on exon 18 of *RPGRIP1* appeared variable among the heterozygotes (Supplemental Figure 4b, I-2, II-1, and II-2). In contrast, genome sequence data can show the break point in the flanking intron (Figure 2B) and indicate a possible deletion between the paired reads (Figure 2B and E, red lines), which helps to reliably detect the variant. Compared with the pathogenic variant identification ratio in cone dysfunctions in our exome sequencing study (34%, 14/41 pedigrees), genome sequencing improved the detection ratio to 50% (22/44). Homozygous *RPGRIP1*-ex18-DEL accounted for 11% (5/44) of the pedigrees diagnosed as cone dysfunctions. Because the previous study did not separate ACHM from other phenotypes of cone dysfunction (blue cone monochromatism and others), the contribution of *RPGRIP1*-ex18-DEL to ACHM in Japanese patients with IRD might be underestimated.

Because *RPGRIP1* is expressed in both rod and cone photoreceptors, the molecular pathology that primarily affects cone photoreceptors in patients has yet to be clarified. Beryozkin et al<sup>11</sup> showed significantly different distributions of LCA and CORD phenotypes corresponding to the *RPGRIP1* genotypes. Homozygous premature terminations were more associated with LCA, whereas homozygous missense variants were preferentially associated with CORD. Because premature terminations are generally



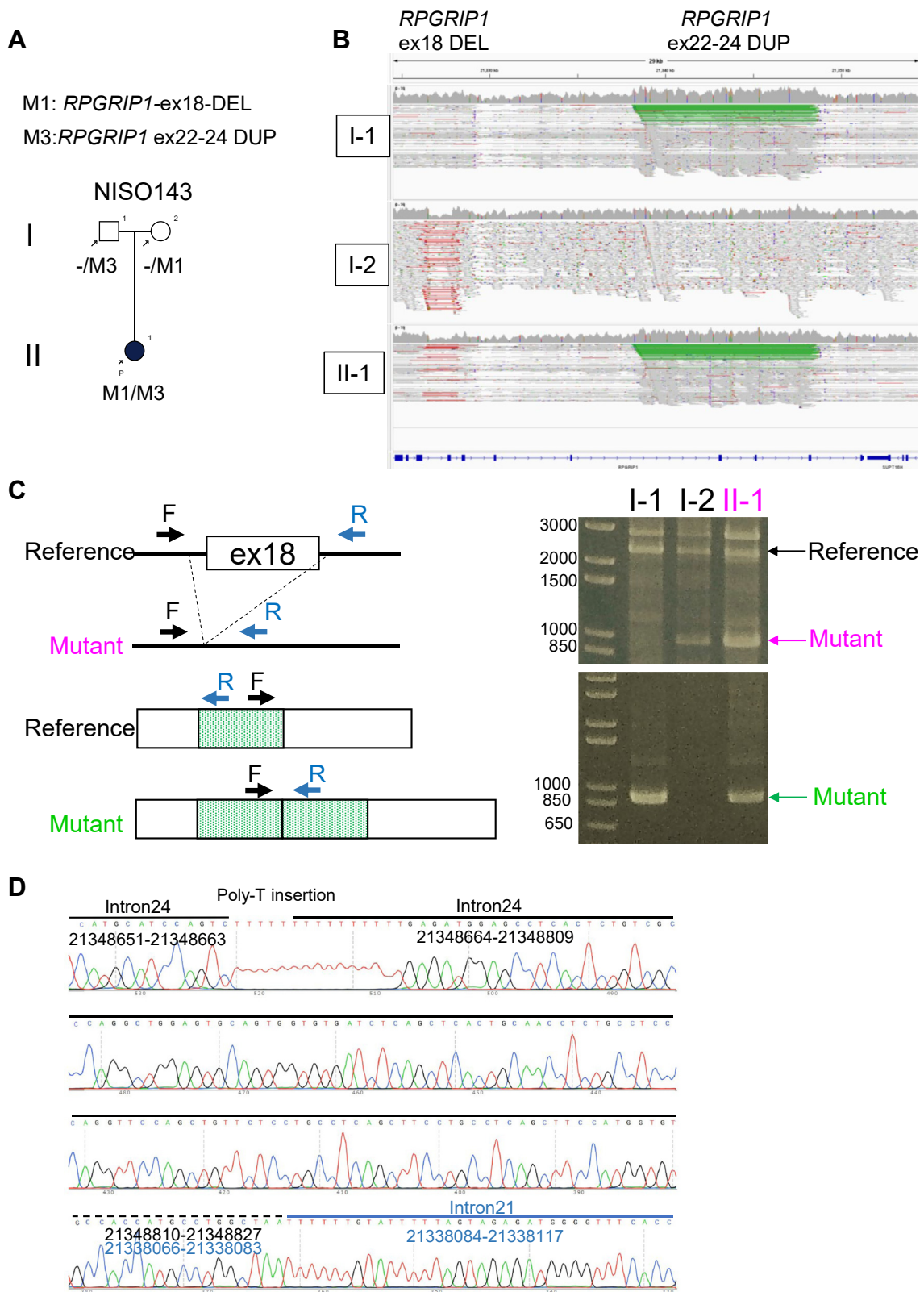


**Figure 3** *RPGRIP1*-ex18-DEL and exons 22-24 duplication in NISO143. **A**. Family tree of NISO143 showing variant inheritance of *RPGRIP1*-ex18-DEL and *RPGRIP1* ex22-24 DUP. **B**. Read alignments. Red lines indicate deletions in read sequences compared with the reference, whereas green lines indicate duplications of the region. **C**. Schematic explanation and PCR band patterns to confirm *RPGRIP1*-ex18-DEL (upper panels) and *RPGRIP1* ex22-24 DUP (lower panels). **D**. Sanger sequencing identifies the break point of *RPGRIP1* ex22-24 DUP using II-1 PCR product. Dotted line indicates 18 bases aligned to both edges of the duplicated region

considered as equal to a null variant, these results suggest a correlation between phenotype severity and variant impact. Although *RPGRIP1*-ex18-DEL is predicted to cause a frameshift and premature termination resulting from the loss of 185 bases of the coding sequence, the exact impact of the deletion of exon 18 with flanking introns on both sides has yet to be tested experimentally. Considering the variable effect of deep-intron variants on RNA splicing,<sup>13,40</sup> large deletions in introns 17 and 18 (1077 and 77 bp, respectively) might cause splicing errors rather than simply connecting the remaining exons. Molecular validation of *RPGRIP1*-ex18-DEL and a novel identified structural variant (*RPGRIP1* ex22-24 DUP) will provide further insights into genotype-phenotype correlations.

At present, there is no clinical treatment for ACHM, but the recessive inheritance pattern and remaining cone photoreceptor cells in patients with ACHM are appropriate for gene supplementation therapy. After the positive results of adeno-associated virus (AAV)-mediated gene supplementation experiments in ACHM animal models (eg, *Cnga3* and *Cngb3* knockout mice),<sup>41,42</sup> multiple clinical studies targeting *CNGA3*- or *CNGB3*-associated ACHM are ongoing or recently completed (NCT03758404, NCT02610582, NCT02935517, NCT03001310, NCT03278873, and NCT02599922). In addition, preclinical studies of gene replacement therapy using AAV-packed mouse *Rpgrip1* cDNA and human *RPGRIP1* cDNA on *Rpgrip1* knockout mice have already been published.<sup>43,44</sup> In both studies, treated eyes showed normal localization of exogenously expressed RPGRIP1 protein, rescue of the photoreceptor outer segment, and recovery of ERG responses. Although these studies rescued the LCA phenotype, these results indicate that AAV-delivered RPGRIP1 can supplement normal RPGRIP1 functions. According to the MAF in the Japanese population and current 2022 population estimates,<sup>45</sup> more than 600 individuals are expected to be homozygous for *RPGRIP1*-ex18-DEL in Japan ( $124,947,000 \times 0.0023^2$ ). The exact effect of the variant remains to be elucidated, but *RPGRIP1* could be a promising clinical target for patients with ACHM in Japan.

In conclusion, we identified a frequent association of *RPGRIP1*-ex18-DEL with the ACHM phenotype in Japanese patients, further contributing to the wide spectrum of *RPGRIP1*-associated IRD phenotypes from LCA to ACHM. Detailed phenotyping and genome sequencing improved the pathogenic variant identification ratio of cone dysfunction syndromes in our cohort from 34% to 50%. Identification of homozygous *RPGRIP1*-ex18-DEL in 5 of 10 patients with ACHM suggests that this variant accounts for a non-negligible portion of Japanese patients with ACHM.

## Data Availability

The raw individual genome sequence data are not publicly available because of the privacy policy. Deidentified data will

be available under the regulation of Japan leading project for rare disease WGS (<https://rare-disease-wgs.jp/en/>).

## Acknowledgments

The authors thank Write Science Right ([www.writesciencerright.com](http://www.writesciencerright.com)) for checking grammatical errors of the manuscript.

## Funding

Support for this work was awarded to K.T. and T.I. by the Japan Agency for Medical Research and Development (AMED) under grant number JP22ek0109493, and awarded to K.T., S.U., and T.H. by the Health Labor Sciences Research Grant (20FC1029).

## Author Information

Conceptualization: A.S., T.I.; Data Curation: A.S., K.M., T.I., K.Y.; Funding Acquisition: T.I., K.Tsunoda, S.U., T.H.; Investigation: A.S., K.Y., N.M., K.M.; Methodology: A.S., K.Tsunoda, T.H., S.U., T.I.; Project Administration: T.I.; Resources: Y.K., Y.O., K.Tokunaga, NCBN Controls WGS Consortium; Supervision: T.I.; Writing-original draft: A.S., K.M.; Writing-review and editing: K.K., K.Tsunoda, K.K., T.H., S.U., T.I.

## ORCIDiDs

Akiko Suga: <https://orcid.org/0000-0001-6609-2647>  
 Kei Mizobuchi: <https://orcid.org/0000-0001-5389-6507>  
 Kazutoshi Yoshitake: <https://orcid.org/0000-0002-8247-9443>  
 Kazuki Kuniyoshi: <https://orcid.org/0000-0003-0242-5662>  
 Yosuke Kawai: <https://orcid.org/0000-0003-0666-1224>  
 Katsushi Tokunaga: <https://orcid.org/0000-0001-5501-0503>  
 Takaaki Hayashi: <https://orcid.org/0000-0002-1535-0279>  
 Shinji Ueno: <https://orcid.org/0000-0001-5716-3626>  
 Takeshi Iwata: <https://orcid.org/0000-0003-1447-0081>

## Ethics Declaration

The study was approved by the ethics board of NHO Tokyo Medical Center (R18-029), and also by the ethics boards of all participating institutions. Recruitment and sample collection were conducted in accordance with the Declaration of Helsinki. All participants provided written informed consent at their respective recruiting institutes.

## Conflict of Interest

The authors declare no conflicts of interest.

## Additional Information

The online version of this article (<https://doi.org/10.1016/j.gimo.2024.101843>) contains supplemental material, which is available to authorized users.

## Affiliations

<sup>1</sup>Division of Molecular and Cellular Biology, National Institute of Sensory Organs, NHO Tokyo Medical Center, Tokyo, Japan; <sup>2</sup>Department of Ophthalmology, The Jikei University School of Medicine, Tokyo, Japan; <sup>3</sup>Department of Ophthalmology, Nagoya University Graduate School of Medicine, Aichi, Japan; <sup>4</sup>Laboratory of Aquatic Molecular Biology and Biotechnology, Aquatic Bioscience, Graduate School of Agricultural and Life Sciences, The University of Tokyo, Tokyo, Japan; <sup>5</sup>Division of Vision Research, National Institute of Sensory Organs, NHO Tokyo Medical Center, Tokyo, Japan; <sup>6</sup>Department of Ophthalmology, Kindai University Faculty of Medicine, Osaka, Japan; <sup>7</sup>Genome Medical Science Project, National Center for Global Health and Medicine, Tokyo, Japan; <sup>8</sup>Department of Ophthalmology, Hirosaki University Graduate School of Medicine, Aomori, Japan

## Members of the NCBN Controls WGS Consortium

Hatsue Ishibashi-Ueda, Tsutomu Tomita, Michio Noguchi, Ayako Takahashi, Yu-ichi Goto, Sumiko Yoshida, Kotaro Hattori, Ryo Matsumura, Aritoshi Iida, Yutaka Maruoka, Hiroyuki Gatanaga, Masaya Sugiyama, Satoshi Suzuki, Kengo Miyo, Yoichi Matsubara, Akihiro Umezawa, Kenichiro Hata, Tadashi Kaname, Kouichi Ozaki, Haruhiko Tokuda, Hiroshi Watanabe, Shumpei Niida, Eisei Noiri14, Koji Kitajima, Yosuke Omae, Reiko Miyahara, Hideyuki Shimanuki, Yosuke Kawai, and Katsushi Tokunaga

## References

- Hirji N, Georgiou M, Kalitzeos A, et al. Longitudinal assessment of retinal structure in achromatopsia patients with long-term follow-up. *Invest Ophthalmol Vis Sci*. 2018;59(15):5735-5744. <http://doi.org/10.1167/iovs.18-25452>
- Hirji N, Aboshiha J, Georgiou M, Bainbridge J, Michaelides M. Achromatopsia: clinical features, molecular genetics, animal models and therapeutic options. *Ophthalmic Genet*. 2018;39(2):149-157. <http://doi.org/10.1080/13816810.2017.1418389>
- Aboshiha J, Dubis AM, Carroll J, Hardcastle AJ, Michaelides M. The cone dysfunction syndromes. *Br J Ophthalmol*. 2016;100(1):115-121. <http://doi.org/10.1136/bjophthalmol-2014-306505>
- Kohl S, Zobor D, Chiang WC, et al. Mutations in the unfolded protein response regulator ATF6 cause the cone dysfunction disorder achromatopsia. *Nat Genet*. 2015;47(7):757-765. <http://doi.org/10.1038/ng.3319>
- Carss KJ, Arno G, Erwood M, et al. Comprehensive rare variant analysis via whole-genome sequencing to determine the molecular pathology of inherited retinal disease. *Am J Hum Genet*. 2017;100(1):75-90. <http://doi.org/10.1016/j.ajhg.2016.12.003>
- Weisschuh N, Obermaier CD, Battke F, et al. Genetic architecture of inherited retinal degeneration in Germany: a large cohort study from a single diagnostic center over a 9-year period. *Hum Mutat*. 2020;41(9):1514-1527. <http://doi.org/10.1002/humu.24064>
- Johnson S, Michaelides M, Aligianis IA, et al. Achromatopsia caused by novel mutations in both CNGA3 and CNGB3. *J Med Genet*. 2004;41(2):e20. <http://doi.org/10.1136/jmg.2003.011437>
- Suga A, Yoshitake K, Minematsu N, et al. Genetic characterization of 1210 Japanese pedigrees with inherited retinal diseases by whole-exome sequencing. *Hum Mutat*. 2022;43(12):2251-2264. <http://doi.org/10.1002/humu.24492>
- Zhao Y, Hong DH, Pawlyk B, et al. The retinitis pigmentosa GTPase regulator (RPGR)-interacting protein: subserving RPGR function and participating in disk morphogenesis. *Proc Natl Acad Sci U S A*. 2003;100(7):3965-3970. <http://doi.org/10.1073/pnas.0637349100>
- Dryja TP, Adams SM, Grimsby JL, et al. Null RPGRIP1 alleles in patients with Leber congenital amaurosis. *Am J Hum Genet*. 2001;68(5):1295-1298. <http://doi.org/10.1086/320113>
- Beryozkin A, Aweidah H, Carrero Valenzuela RD, et al. Retinal degeneration associated with RPGRIP1: a review of natural history, mutation spectrum, and genotype-phenotype correlation in 228 patients. *Front Cell Dev Biol*. 2021;9:746781. <http://doi.org/10.3389/fcell.2021.746781>
- Huang CH, Yang CM, Yang CH, Hou YC, Chen TC. Leber's congenital amaurosis: current concepts of genotype-phenotype correlations. *Genes (Basel)*. 2021;12(8):1261. <http://doi.org/10.3390/genes12081261>
- Jamshidi F, Place EM, Mehrotra S, et al. Contribution of noncoding pathogenic variants to RPGRIP1-mediated inherited retinal degeneration. *Genet Med*. 2019;21(3):694-704. <http://doi.org/10.1038/s41436-018-0104-7>
- Iwata T. Japan to Global Eye Genetics Consortium: extending research collaboration for inherited eye diseases. *Asia Pac J Ophthalmol (Phila)*. 2022;11(4):360-368. <http://doi.org/10.1097/APO.0000000000000535>
- Robson AG, Frishman LJ, Grigg J, et al. ISCEV Standard for full-field clinical electroretinography (2022 update). *Doc Ophthalmol*. 2022;144(3):165-177. <http://doi.org/10.1007/s10633-022-09872-0>
- Katagiri S, Hayashi T, Kondo M, et al. RPE65 mutations in two Japanese families with Leber congenital amaurosis. *Ophthalmic Genet*. 2016;37(2):161-169. <http://doi.org/10.3109/13816810.2014.991931>
- Mizobuchi K, Hayashi T, Ohira R, Nakano T. Electroretinographic abnormalities in Alport syndrome with a novel COL4A5 truncated variant (p.Try20GlyfsTer19). *Doc Ophthalmol*. 2023;146(3):281-291. <http://doi.org/10.1007/s10633-023-09935-w>
- Hayashi T, Gekka T, Goto-Omoto S, Takeuchi T, Kubo A, Kitahara K. Novel NR2E3 mutations (R104Q, R334G) associated with a mild form of enhanced S-cone syndrome demonstrate compound heterozygosity. *Ophthalmology*. 2005;112(12):2115. <http://doi.org/10.1016/j.ophtha.2005.07.002>
- Kato K, Kondo M, Sugimoto M, Ikesugi K, Matsubara H. Effect of pupil size on flicker ERGs recorded with RETeval system: new mydriasis-free full-field ERG system. *Invest Ophthalmol Vis Sci*. 2015;56(6):3684-3690. <http://doi.org/10.1167/iovs.14-16349>
- Tokutomi T, Fukushima A, Yamamoto K, Bansho Y, Hachiya T, Shimizu A. f-treeGC: a questionnaire-based family tree-creation software for genetic counseling and genome cohort studies. *BMC Med Genet*. 2017;18(1):71. <http://doi.org/10.1186/s12881-017-0433-4>
- Kawai Y, Watanabe Y, Omae Y, et al. Exploring the genetic diversity of the Japanese population: insights from a large-scale whole genome sequencing analysis. *PLoS Genet*. 2023;19(12):e1010625. <http://doi.org/10.1371/journal.pgen.1010625>
- RDWGS. Accessed December 7, 2023. <https://rare-disease-wgs.jp/en/>

23. Li H, Durbin R. Fast and accurate short read alignment with Burrows-Wheeler transform. *Bioinformatics*. 2009;25(14):1754-1760. <http://doi.org/10.1093/bioinformatics/btp324>
24. Franke KR, Crowgey EL. Accelerating next generation sequencing data analysis: an evaluation of optimized best practices for Genome Analysis Toolkit algorithms. *Genomics Inform*. 2020;18(1):e10. <http://doi.org/10.5808/GI.2020.18.1.e10>
25. Wang K, Li M, Hakonarson H. ANNOVAR: functional annotation of genetic variants from high-throughput sequencing data. *Nucleic Acids Res*. 2010;38(16):e164. <http://doi.org/10.1093/nar/gkq603>
26. Jaganathan K, Kyriazopoulou Panagiotopoulou S, McRae JF, et al. Predicting splicing from primary sequence with deep learning. *Cell*. 2019;176(3):535-548.e24. <http://doi.org/10.1016/j.cell.2018.12.015>
27. Collins RL, Brand H, Karczewski KJ, et al. A structural variation reference for medical and population genetics. *Nature*. 2020;581(7809):444-451. <http://doi.org/10.1038/s41586-020-2287-8>
28. Gardner EJ, Lam VK, Harris DN, et al. The Mobile Element Locator Tool (MELT): population-scale mobile element discovery and biology. *Genome Res*. 2017;27(11):1916-1929. <http://doi.org/10.1101/gr.218032.116>
29. Otsuki A, Okamura Y, Ishida N, et al. Construction of a trio-based structural variation panel utilizing activated T lymphocytes and long-read sequencing technology. *Commun Biol*. 2022;5(1):991. <http://doi.org/10.1038/s42003-022-03953-1>
30. Li Q, Wang K. InterVar: clinical interpretation of genetic variants by the 2015 ACMG-AMP guidelines. *Am J Hum Genet*. 2017;100(2):267-280. <http://doi.org/10.1016/j.ajhg.2017.01.004>
31. Geoffroy V, Herenger Y, Kress A, et al. AnnotSV: an integrated tool for structural variations annotation. *Bioinformatics*. 2018;34(20):3572-3574. <http://doi.org/10.1093/bioinformatics/bty304>
32. Robinson JT, Thorvaldsdóttir H, Winckler W, et al. Integrative genomics viewer. *Nat Biotechnol*. 2011;29(1):24-26. <http://doi.org/10.1038/nbt.1754>
33. Suzuki T, Fujimaki T, Yanagawa A, et al. A novel exon 17 deletion mutation of RPGRIP1 gene in two siblings with Leber congenital amaurosis. *Jpn J Ophthalmol*. 2014;58(6):528-535. <http://doi.org/10.1007/s10384-014-0339-z>
34. Wheeler TJ, Clements J, Eddy SR, et al. Dfam: a database of repetitive DNA based on profile hidden Markov models. *Nucleic Acids Res*. 2013;41(database issue):D70-D82. <http://doi.org/10.1093/nar/gks1265>
35. Khan AO, Abu-Safieh L, Eisenberger T, Bolz HJ, Alkuraya FS. The RPGRIP1-related retinal phenotype in children. *Br J Ophthalmol*. 2013;97(6):760-764. <http://doi.org/10.1136/bjophthalmol-2012-303050>
36. Torii K, Nishina S, Morikawa H, et al. The structural abnormalities are deeply involved in the cause of RPGRIP1-related retinal dystrophy in Japanese patients. *Int J Mol Sci*. 2023;24(18):13678. <http://doi.org/10.3390/ijms241813678>
37. Ueno S, Nakanishi A, Sayo A, et al. Differences in ocular findings in two siblings: one with complete and other with incomplete achromatopsia. *Doc Ophthalmol*. 2017;134(2):141-147. <http://doi.org/10.1007/s10633-017-9577-y>
38. Khan AO. RPGRIP1-related retinal disease presenting as isolated cone dysfunction. *Ophthalmic Genet*. 2023;44(6):595-597. <http://doi.org/10.1080/13816810.2023.2175224>
39. Miyamichi D, Nishina S, Hosono K, et al. Retinal structure in Leber's congenital amaurosis caused by RPGRIP1 mutations. *Hum Genome Var*. 2019;6:32. <http://doi.org/10.1038/s41439-019-0064-8>
40. Bauwens M, Garanto A, Sangermano R, et al. ABCA4-associated disease as a model for missing heritability in autosomal recessive disorders: novel noncoding splice, cis-regulatory, structural, and recurrent hypomorphic variants. *Genet Med*. 2019;21(8):1761-1771. <http://doi.org/10.1038/s41436-018-0420-y>
41. Michalakakis S, Mühlfriedel R, Tanimoto N, et al. Restoration of cone vision in the CNGA3<sup>-/-</sup> mouse model of congenital complete lack of cone photoreceptor function. *Mol Ther*. 2010;18(12):2057-2063. <http://doi.org/10.1038/mt.2010.149>
42. Carvalho LS, Xu J, Pearson RA, et al. Long-term and age-dependent restoration of visual function in a mouse model of CNGB3-associated achromatopsia following gene therapy. *Hum Mol Genet*. 2011;20(16):3161-3175. <http://doi.org/10.1093/hmg/ddr218>
43. Pawlyk BS, Smith AJ, Buch PK, et al. Gene replacement therapy rescues photoreceptor degeneration in a murine model of Leber congenital amaurosis lacking RPGRIP. *Invest Ophthalmol Vis Sci*. 2005;46(9):3039-3045. <http://doi.org/10.1167/iovs.05-0371>
44. Pawlyk BS, Bulgakov OV, Liu X, et al. Replacement gene therapy with a human RPGRIP1 sequence slows photoreceptor degeneration in a murine model of Leber congenital amaurosis. *Hum Gene Ther*. 2010;21(8):993-1004. <http://doi.org/10.1089/hum.2009.218>
45. Current population estimates as of October 1, 2022. Statistics Bureau of Japan. Accessed October 10, 2023. <https://www.stat.go.jp/english/data/jinsui/2022np/index.html>